Skeletal Radiology (2020) 49:1567–1579
https://doi.org/10.1007/s00256-020-03438-4

SCIENTIFIC ARTICLE

Traumatic injury of the triangular fibrocartilage complex (TFCC) —a refinement to the Palmer classification by using high-resolution 3-T MRI

Huili Zhan[1] · Rongjie Bai[1] · Zhanhua Qian[1] · Yong Yang[2] · Heng Zhang[1] · Yuming Yin[3]

Received: 21 December 2019 / Revised: 30 March 2020 / Accepted: 31 March 2020 / Published online: 5 May 2020

Abstract

Objective The aim of this study was to investigate the MR features of the traumatic injury of the triangular fibrocartilage complex (TFCC) by using high-resolution 3-T magnetic resonance imaging (MRI) and to refine the Palmer classification system.

Materials and methods From November 2015 to May 2019, sixty-seven patients met the including and excluding criteria and were enrolled into this retrospective study. All subjects had high-resolution 3-T MRI scan of the wrist and eleven had indirect MR arthrography of the wrist. All the MRI were read by two experienced musculoskeletal radiologists. Diagnostic sensitivity, specificity, and accuracy of MRI were calculated by using the arthroscopy and surgery as the standard of reference. A *P* value less than 0.05 was considered statistically significant. The interobserver agreement was assessed by kappa analysis.

Results There were 49 cases of TFCC injuries proven by the arthroscopy or surgery. The TFCC injuries in the other 18 patients were proved by the combination of clinical follow-up examination and follow-up MRI. Among the arthroscopy- or surgery-confirmed cases, there were 32 patients with original Palmer injuries (IA = 10, IB = 19, ID = 3), 5 with capsular detachment, 4 with bucket-handle tear of the TFCC that have rarely been reported, and 8 with complex injuries that involved the listed classifications above. The sensitivities and specificities of MRI for diagnosing IA, IB, ID, complex injuries, and bucket-handle tear were 67–100% and 90–100%, and overall good to perfect interobserver agreements (kappa, 0.64–1.00). The diagnostic performance for the capsular detachment was lower (kappa, 0.38).

Conclusion With high-resolution 3-T MRI, more detailed injury patterns were found including capsular injuries, the horizontal tear of the articular disk, and the bucket-handle tear. It is necessary to refine the classic Palmer classification of TFCC injuries.

Keywords Traumatic · Triangular fibrocartilage complex (TFCC) · Injury · Magnetic resonance imaging · Classification

Introduction

The triangular fibrocartilage complex (TFCC) is an important structure to maintain the stability of the ulnocarpal joint and the distal radioulnar joint (DRUJ) and allow the stable motion of the wrist and the rotation of the forearm [1–7]. The original Palmer classification of TFCC injuries has gained widespread acceptance by radiologists and hand surgeons since it was published in 1989 and still serves as a reference in the diagnosis and treatment for traumatic TFCC injury. Traumatic TFCC injuries in the original Palmer classification system are categorized into four different types according to the injury location. However, with further understanding of the anatomy and biomechanics of TFCC and DRUJ and the advanced imaging techniques, more injury types have been found that were not included in the original Palmer classification. We feel it is necessary to refine the original Palmer classification to provide a more comprehensive injury spectrum for clinicians.

Some authors stated that computed tomography (CT) with arthrography was more sensitive than MRI in the diagnosis of tears of the TFCC, especially for central perforation [8, 9]. However, it is generally believed that MRI and MR

✉ Rongjie Bai
bairongjie@126.com

[1] Department of Radiology, Beijing Jishuitan Hospital, Peking University Fourth School of Clinical Medicine, No. 31, Xinjiekou East St, Xicheng District, Beijing 100035, China

[2] Department of Hand Surgery, Beijing Jishuitan Hospital, No. 31, Xinjiekou East St, Xicheng District, Beijing 100035, China

[3] Radiology Associates, LLP, 1814 South Alameda Street, Corpus Christi, TX 78404, USA

arthrography are equal if not superior to CT arthrography in detecting TFC injury. More associated injuries can also be detected with MRI, such as adjacent soft tissue injuries, articular cartilage injuries, and acute bone contusion. According to our previous study [10], high-resolution 3-T magnetic resonance imaging (MRI) is capable to show the complex details of the TFCC anatomy. In our current study, we have found several injury patterns that were not included in the original Palmer classification. We hypothesized that with high-resolution MRI, more injury patterns can be demonstrated. Some of these TFCC injury patterns may be associated with instability of the DRUJ or ulnocarpal joint, which may further influence the clinical management. Thus, this research was designed to illustrate the MR features of various TFCC injury patterns and provide a detailed and integrated classification system to further refine the Palmer classification.

Materials and methods

This research protocol was reviewed and approved by the institutional ethic review board.

Study population

To be included in this study, all patients with TFCC injuries had a history of traumatic injury of the wrist and all presented with ulnar-sided wrist pain. All of the patients had either surgery or complete follow-up data. Patients having any of the following conditions will be excluded from this study: Palmer type II degenerative tears (including type I coupled with type II), inflammatory arthritis, tumor or tumor-like lesions, deformity of the wrist (such as Madelung deformity), or previous history of wrist surgery. From November 2015 to May 2019, sixty-seven patients met the including and excluding criteria and were enrolled into this retrospective study. Forty-nine patients had wrist arthroscopy or surgery with the interval range from 4 days to 13 months after the MR imaging examinations. The remaining 18 patients accepted the conservative treatment with a follow-up period that ranged from 3 to 12 months.

MR imaging

Magnetic resonance imaging was performed with a 3-T MR imaging unit (Philips Achieva, Philips Medical Systems Nederland B.V., P.O. Box 10000, 5680 DA Best, The Netherlands) with a 16-channel hand-and-wrist receiver-only coil (Philips Hand/Wrist 16 3-T Tim coil, model (IT)). All patients were placed in prone position and the examined arms were raised above the head, so that the wrist can be in the isocenter of the scanner bore pinpointed by the laser mark. Immediately after the unenhanced MR examination, 11 patients who were suspected with ulnar-sided attachment injury of the TFC during the clinical examination had indirect wrist arthrogram.

The magnetic resonance imaging sequences include fat-suppressed proton density (PD FS)–weighted imaging in axial, coronal, and sagittal planes (TR/TE 2500–2609/35), and T1-weighted fast spin-echo in coronal plane (TR/TE 326/15, slice thickness, 2–3 mm; interslice space, 0.2–0.3 mm; NEX, 2–4; field of view, 80–90 × 80–90 mm; and voxel, (0.25–0.31)mm × (0.35–0.45)mm × (2.0–2.8)mm).

Eleven patients had indirect wrist arthrography with intravenous (IV) injection of gadopentetate dimeglumine 9.38 g/20 mL (Beilu Pharmaceutical Co. Ltd., Beijing, China), 0.2 mL/kg body weight, and maximum volume of 20 mL. Those patients were kept still on the scanner table for 10 min after the contrast injection through an IV access in the opposite arm. Then, the second scan was performed with the following additional sequences: T1-weighted fat-saturated (T1 FS) imaging in the axial, coronal, and sagittal planes (TR/TE 378/15, slice thickness, 2–3 mm; interslice space, 0.2–0.3 mm; NEX, 2–4; field of view, 80–90 × 80–90 mm; and voxel, (0.28–0.30)mm × (0.39–0.43)mm × (2.0–3.0)mm).

MR imaging analysis

All the MRI were read retrospectively by two senior musculoskeletal radiologists with 5 to 10 years of experience. The discrepancies were resolved by consensus by introducing an additional musculoskeletal radiologist with more than 10 years of experience. The MR examinations were presented to the reviewers in a random order in order to avoid bias, and both reviewers were blinded to all clinical data including surgery reports and the follow-up data. The appearance of TFCC and signal intensity on MR images of the 67 patients were analyzed. If there were discontinuity of fibers and abnormal increase in signal intensity extending to both superior and inferior surfaces on FS PD images, we defined it as a complete tear, whereas if there was discontinuity of some fibers with some continuity, a partial tear could be diagnosed. Based on the modified classification system presented in a previous article (Fig. 1) [10], we present a comprehensive classification of TFCC injuries (Table 1). According to the new classification, the readers then were asked to further evaluate the presence or absence of foveal insertion tear, styloid insertion tear, complete tear of the ulnar attachment of the TFC, fracture of the ulnar styloid without tear of the foveal insertion or styloid insertion, fracture of the ulnar styloid with foveal insertion tear, “floating styloid,” fibrocartilage-radius interface tear, dorsal or volar rim tear, and radial interface tear with/without dorsal or volar rim tear. If a patient had more than one type of injury, the injury patterns will only be classified as complex injuries instead of classifying in detail. The MR imaging features of different subtypes of the injuries were

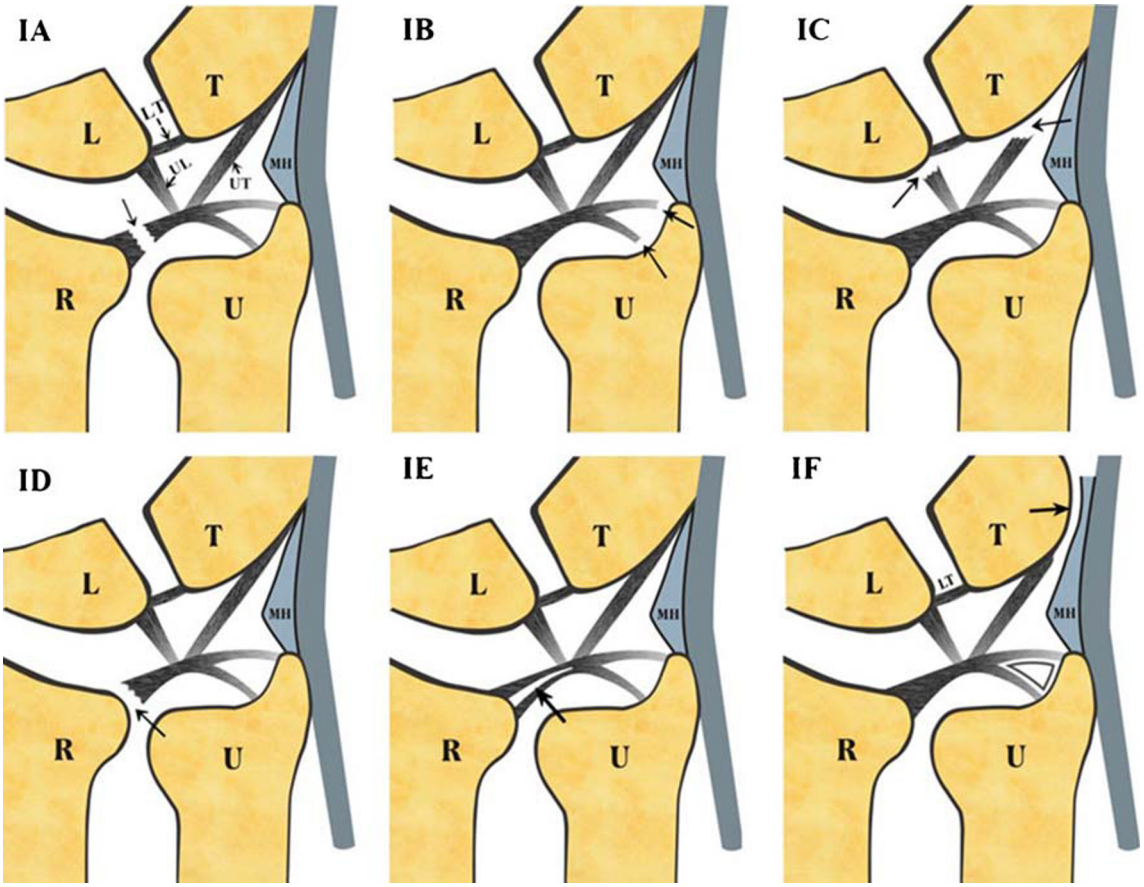

Fig. 1 Modified classification of traumatic Palmer TFCC injuries. Schematic drawing of the modified traumatic classification showed the traumatic TFCC injuries could be categorized as central perforation, ulnar avulsion, distal avulsion, radial avulsion, horizontal tear, and capsular detachment according to the location. L, lunate; T, triquetrum; R, radius; U, ulna; LT, lunotriquetral ligament; UT, ulnotriquetral ligament; UL, ulnolunate ligament; MH, meniscus homologue

compared with the arthrographic findings, surgical results, and follow-up data in a double-blind manner.

Statistical analysis

For all statistical calculations, statistical software MedCalc version 16.8.4 (Ostend, Belgium) was used. Descriptive statistics were used for demographics to describe the numbers and percentages of patients. For assessing agreement among the two observers, weighted kappa values were calculated; kappa values of 0–0.20 indicate poor agreement, 0.21–0.40, fair agreement; 0.41–0.60, moderate agreement; 0.61–0.80, substantial agreement; and 0.81–1.00, almost perfect agreement. The diagnostic performance of MRI was determined by calculating sensitivity and specificity with arthroscopic or surgery serving as the standard of reference. The area under the (AUC) receiver operating characteristic (ROC) curve was used to define test accuracy (0.9–1, excellent; 0.8–0.9, good; 0.7–0.8, fair; 0.6–0.7, poor; 0.5–0.6, fail). A P value less than 0.05 was considered statistically significant.

Results

Traumatic TFCC injuries

There were 67 patients—33 males and 34 females—with the age ranging from 11 to 60 years. There were 49 cases of TFCC injuries proven by arthroscopy or surgery. The diagnosis of the rest of the 18 cases was established by initial imaging findings, clinical data, and follow-up examinations, with follow-up period ranging from 3 to 12 months. One of the important findings in acute traumatic TFCC injury is increased FS PD signal within the injured TFCC and adjacent tissue, representing a tear or strain and tissue edema. During the course of follow-up, MR images of patients with conservative treatment showed abnormally high signal intensity that decreased on FS PD-weighted images and the swelling of tissue was reduced. Among the 49 patients with arthroscopy- or surgery-confirmed traumatic TFCC injuries, there were 32 patients with original Palmer injuries (IA = 10, IB = 19, ID = 3), 5 with capsular detachment, and 4 with bucket-handle tear of the TFCC. The bucket-handle tear of the TFCC has rarely been reported. There were 8 patients with

Table 1 The refined Palmer classification of traumatic TFCC injuries

IA Central perforation	IB Ulnar-side injury	IC Distal avulsion	ID Radial side avulsion	IE Horizontal tear of the articular disk	IF Capsular detachment	IG Bucket-handle tear of the TFCC
	(1) Ulnar attachment injuries of the TFC IB1. Foveal insertion tear IB2. Styloid insertion tear IB3. Complete avulsion IB4. Stable pseudoarthrosis IB5. Unstable pseudoarthrosis IB6. "Floating styloid" (2) Miscellany Ulnomeniscal homologue tear ECU injury		ID1. Fibrocartilage-radius interface tear ID2. Dorsal/volar rim tear ID3. Fibrocartilage tear + dorsal/volar rim avulsion with/without avulsion fracture of the sigmoid notch of the radius ID4. Complete detachment		IF1.Volar capsular TFC detachment IF2. Dorsal capsular TFC detachment IF3. Dorsal capsular detachment from the triquetral insertion IF4. Dorsal capsular TFC detachment and detachment from the triquetral insertion	

complex type of injuries that involved more than one listed classifications above.

During MRI interpretation, the radiologists diagnosed IA, IB, ID, complex injuries, and bucket-handle tear with sensitivities of 67–100%, specificities of 90–100%, and overall good to perfect interobserver agreements (kappa, 0.64–1.00) (Table 2). However, the performance for diagnosing the capsular detachment was lower (kappa, 0.38).

Among the 67 patients either confirmed by arthroscopy/surgery or follow-up data, 33 patients had Palmer IB injuries (19 with arthroscopy or surgery, 14 with follow-up data) including the following: IB1 = 13, foveal insertion tear (detachment of the ulnar foveal insertion of the TFC); IB2 = 4, styloid insertion tear (detachment of the ulnar styloid insertion of the TFC); IB3 = 8, complete tear of the ulnar attachment of the TFC (detachment of both the foveal and the styloid insertions of the TFC); IB4 = 2, fracture of the ulnar styloid without tear of the foveal insertion or styloid insertion; IB5 = 3, fracture of the ulnar styloid coupled with foveal insertion tear; IB6 = 3, floating styloid. Three patients had Palmer IB injury also with extensor carpi ulnaris (ECU) tendon injury. One patient had combination of Palmer IB injury with meniscus homologue (MH) injury. However, among these IB injuries, there were only 9 with foveal insertion tear, 5 with complete tear of the ulnar attachment, 3 with fracture of the ulnar styloid coupled with foveal insertion tear, and 2 with "floating styloid" that were proven by arthroscopy or surgery.

Palmer ID injuries were rare. There were only 3 patients proven by the arthroscopy or surgery, including two with tear between the hyaline cartilage of the sigmoid notch of the radius and TFC, and one with radial TFC tear and volar avulsion of the TFCC from the radial sigmoid notch and avulsion fracture of the sigmoid notch.

There were four cases with bucket-handle tears of the TFCC confirmed by arthroscopy or surgery, among them two with different extents of distal radioulnar ligament tears and the fragment located between the proximal carpal bones and the TFC, and the other two with fragment flipped into the prestyloid recess or the DRUJ.

MR features of the ulnar-side traumatic TFCC injuries

IB1. Foveal insertion tear (9 cases with arthroscopic or surgical proven, 4 with non-surgical) Attachment of the proximal lamina to the fovea is injured (Fig. 2). The lamina of the TFC to the styloid insertion is intact. The lesion could be best appreciated on coronal FS PD images (Fig. 2). On MR images, the TFC ulnar foveal attachment shows discontinuity with irregular high signal intensity. This type of injury cannot be detected in the standard arthroscopy of the radiocarpal joint directly. Arthroscopy of the DRUJ would be ideal to assess the proximal component of the TFCC. In addition, the surgeons often judge the tear of foveal insertion by a manual test such as the hook test. Foveal

Table 2 Arthroscopic-based 3-T MRI for the diagnosis of traumatic TFCC injuries

TFCC injury pattern	Reader	Kappa	TP	FN	TN	FP	Sensitivity	Specificity	AUC ROC	*P* value
IA Central perforation (prevalence 10/49, 20%)	R1	0.86 (0.68–1.00)	9	1	38	1	90% (55.5–99.9%)	97% (86.5–99.9%)	0.84 (0.83–0.99)	$P < 0.0001$
	R2		8	2	39	0	80% (44.4–97.5%)	100% (91.0–100%)	0.90 (0.79–0.97)	$P < 0.0001$
IB Ulnar-side injury (prevalence 19/49, 39%)	R1	0.88(0.74–1.00)	19	0	27	3	100% (82.4–100%)	90% (73.5–97.9%)	0.95 (0.85–0.99)	$P < 0.0001$
	R2		18	1	29	1	95% (74.0–99.9%)	97% (82.8–99.9%)	0.96 (0.86–0.99)	$P < 0.0001$
ID Radial side avulsion (prevalence 3/49, 6%)	R1	1.00 (1.00–1.00)	2	1	46	0	67% (9.4–99.2%)	100% (92.3–100%)	0.83 (0.70–0.92)	$P = 0.0455$
	R2		2	1	46	0	67% (9.4–99.2%)	100% (92.3–100%)	0.83 (0.70–0.92)	$P = 0.0455$
Compound injuries (prevalence 8/49, 16%)	R1	0.64 (0.36–0.93)	7	1	39	2	88% (47.3–99.7%)	95% (83.5–99.4%)	0.91 (0.80–0.98)	$P < 0.0001$
	R2		7	1	40	1	88% (47.3–99.7%)	98% (87.1–99.9%)	0.93 (0.81–0.98)	$P < 0.0001$
Capsular detachment (prevalence 5/49, 10%)	R1	0.38 (−0.15–0.91)	1	4	44	0	20% (0.5–71.6%)	100% (92.0–100%)	0.60 (0.45–0.74)	$P = 0.3173$
	R2		4	1	44	0	80% (28.4–99.5%)	100% (92.0–100%)	0.90 (0.78–0.97)	$P = 0.0001$
Bucket-handle tear (prevalence 4/49, 8%)	R1	1.00 (1.00–1.00)	3	1	45	0	75% (19.4–99.4%)	100% (92.1–100%)	0.88 (0.75–0.95)	$P = 0.0027$
	R2		3	1	45	0	75% (19.4–99.4%)	100% (92.1–100%)	0.88 (0.75–0.95)	$P = 0.0027$

TP true positive, *FN* false negative, *TN* true negative, *FP* false positive, *AUC ROC* area under the receiver operating curve

detachment is associated with DRUJ instability, and if required, treatment is reattachment.

IB2. Styloid insertion tear (4 cases with non-surgical proven) It represents the tear of the distal lamina of the TFC in the styloid insertion with or without DRUJ instability. It is characterized by the discontinuity of the distal lamina with increased signal intensity (Fig. 3). The lesion could be best appreciated on coronal FS PD images.

IB3. Complete tear of the ulnar attachment of the TFC (5 cases with arthroscopic or surgical proven, 3 cases with non-surgical) It involves both the foveal and the styloid insertions of the TFC and shows the irregular high signal intensity (Fig. 4). The lesion could be best appreciated on coronal FS PD images and it would be more clearly demonstrated on MR arthrography T1 FS images (Fig. 4). Other signs may include altered morphology, focal synovitis, and fluid accumulation. The complete tear is typically associated with the DRUJ instability. Theoretically, it may require foveal refixation of the TFCC if treatment is indicated.

IB4. Stable pseudoarthrosis (2 cases with non-surgical) It refers to fracture of the ulnar styloid without tear of the foveal insertion or styloid insertion of the TFCC (Fig. 5). On MR images, there is a non-union fracture of the ulnar styloid, and the triangular ligaments are normal. In this type of injury, there is no further treatment required.

IB5. Unstable pseudoarthrosis (3 cases with arthroscopic or surgical proven) It involves a fracture of the ulnar styloid with foveal insertion tear of the TFCC. The lesion could be best appreciated on coronal FS PD images (Fig. 6). It showed the non-union fracture of the ulnar styloid with the increased signal intensity in the foveal insertion of the TFC. In the acute phase, there was bone marrow edema in the ulnar styloid process and fovea and fascial edema. If there is an unstable pseudoarthrosis, the stability of DRUJ should also be evaluated. And if there is a large ulnar styloid fracture contributing to DRUJ instability, surgical fixation is needed.

IB6. "Floating styloid" (2 cases with arthroscopic or surgical proven, 1 case with non-surgical) It demonstrates a displacement of the non-union fracture of the ulnar styloid with a

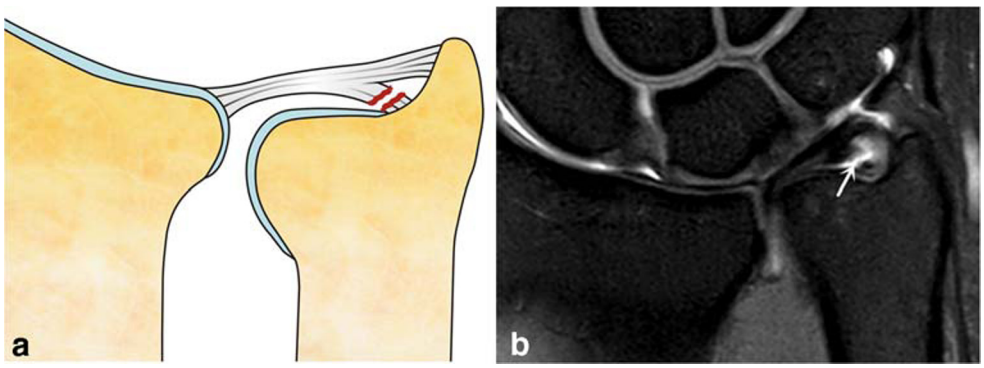

Fig. 2 IB1. Foveal insertion tear. **a** Illustration drawing of IB foveal insertion tear showing the proximal detachment from the foveal insertion. **b** A 40-year-old male with wrist injury. Coronal FS PD-weighted image showed the foveal insertion complete tear which presented as high signal intensity and some fluid accumulation (arrow). FS, fat suppression

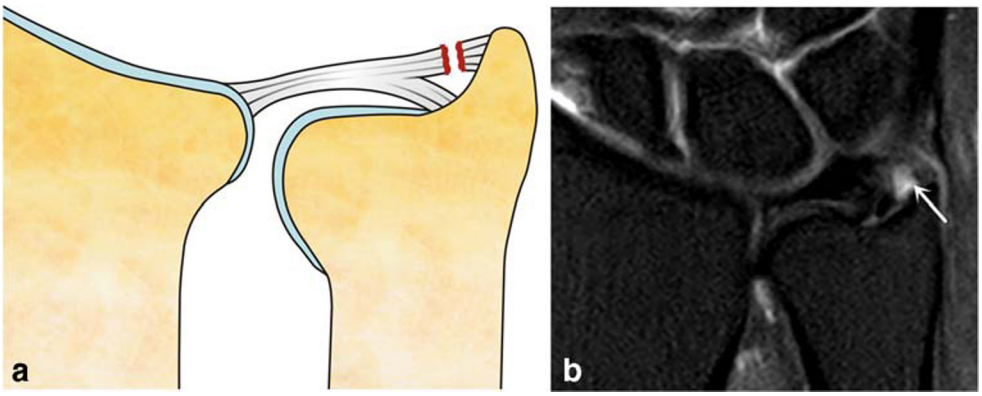

Fig. 3 IB2. Styloid insertion tear. **a** Schematic drawing of IB styloid insertion tear showed the detachment of the ulnar styloid insertion of the TFC. **b** A 30-year-old female with wrist injury. Coronal FS PD-weighted image showed the discontinuity of the distal lamina with irregular high signal intensity in the styloid insertion (arrow). FS, fat suppression

complete tear of the ulnar insertion of the TFC. The lesion could be best appreciated on coronal FS PD images (Fig. 7). In this condition, the styloid may require excision.

Meniscus homologue injury On FS PD images, meniscal homologue injury appears as the increased signal intensity (Fig. 8), and the avulsion of MH from the ulnar attachment or the triquetral attachment and the extent of injury could be appreciated on the coronal plane.

Extensor carpi ulnaris tendon injury On MR images, the ECU tendon would show as the linear or diffuse high signal intensity within the tendon, enlargement of the tendon, tenosynovitis, and fascial edema (Fig. 9). The lesion could be best appreciated on coronal and axial FS PD images.

MR features of traumatic radial side TFCC injuries

The radial side tear of the TFCC is uncommon and the demonstration of the MR features is rare. Because the dorsal or volar rim tear of the TFCC radial attachment is related with the instability of DRUJ and the treatment depends on the tear location, according to the location of abnormal findings, we recommended adding this type of injury to refine the original Palmer classification system (Table 1, Fig. 10).

ID1. Fibrocartilage-radius interface tear (2 cases with arthroscopy or surgery proven, 1 case with non-surgical) It occurs between the hyaline cartilage of the sigmoid notch of the radius and TFCC (Fig. 11). The radial slit or flap interface tear is the most commonly seen. On MR images, it demonstrates as the irregular linear high signal intensity limited to the fibrocartilage area, best seen on consecutive coronal FS PD images and sometimes also on axial images. In our study, there was one patient who had interface tear with peripheral retraction (Fig. 11).

ID3. ID1 tear + volar rim tear + avulsion fracture (1 case with surgery proven) It is a combination injury including the fibrocartilage-radius interface tear and the volar rim avulsion of the TFCC with avulsion fracture of the sigmoid notch of the radius (Fig. 12). On MR images, it shows as the discontinuity and increased signal of the volar distal radioulnar ligament, the high signal intensity of the radial attachment of the TFC, and the fracture and bone marrow edema of the radial sigmoid notch (Fig. 12). The rim tear should be repaired because of the

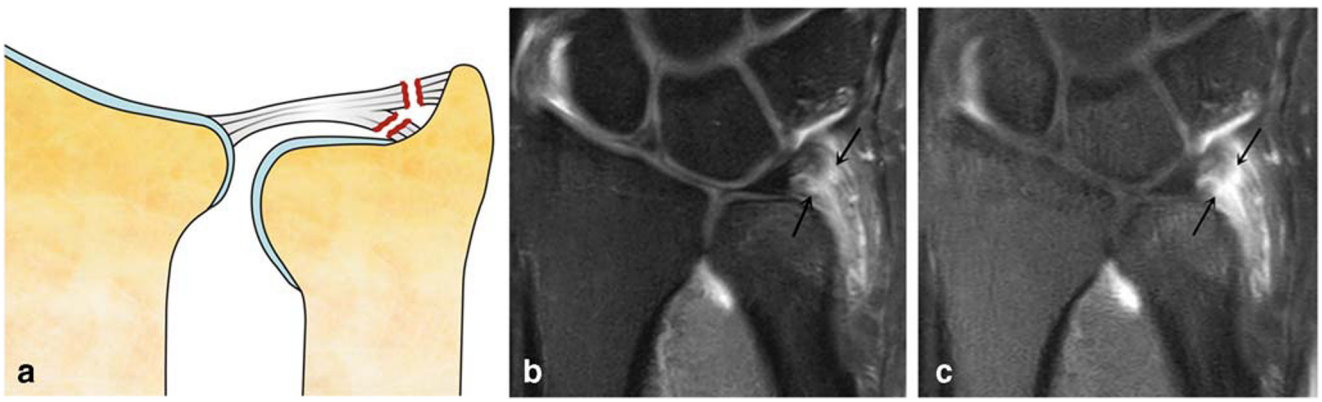

Fig. 4 IB3. Complete tear. **a** Illustration of IB complete tear showed the detachment of both the fovea and the styloid insertions of the TFC. A 45-year-old male with wrist injury. **b** Coronal FS PD-weighted image and **c** coronal T1 FS image after contrast injection showed both the fovea and the styloid insertions of the TFC were partially torn with irregular high signal intensity (arrow) and focal synovitis. It was demonstrated more clearly on the indirect arthrogram. FS, fat suppression

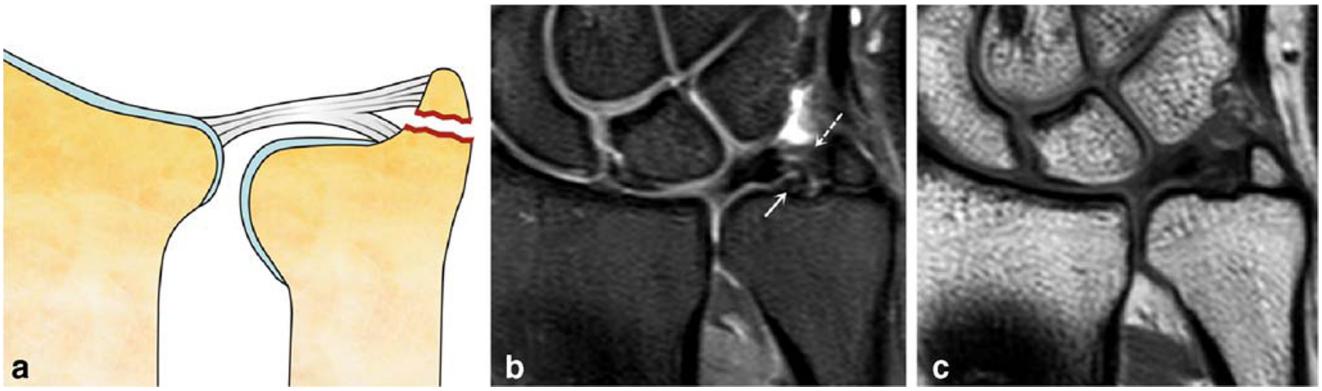

Fig. 5 IB4. Stable pseudoarthrosis. **a** Schematic drawing of IB stable pseudoarthrosis showed the fracture of the ulnar styloid without tear of the foveal insertion or the styloid insertion. A 38-year-old male with wrist injury. **b** Coronal FS PD-weighted image and **c** T1-weighed image showed the non-union at the base of the ulnar styloid process with the proximal lamina (arrow in **b**) and distal lamina (dashed arrow in **b**) remains normal. FS, fat suppression

importance to the DRUJ stability and the fragment of the sigmoid notch needs to be fixed.

MR features of bucket-handle tear of the TFCC

The bucket-handle tear of the TFCC is very rare and has only been seen in case reports in the literatures. The MR features have not been fully described. In our study, we have two cases with bucket-handle tears that have not been reported previously. It occurred in the radial side of the TFCC with partial separation of both the dorsal and volar distal radioulnar ligaments from the articular disk. One has a separated part lifted up like a handle (Fig. 13a). The other one has the radial fragment flipped between the proximal lunate and triquetrum and the preserved articular disk. It could be best evaluated in coronal and sagittal FS PD images (Fig. 13b–d).

Discussion

The Palmer classification has been widely used by hand surgeons and in the musculoskeletal radiologist community. It helped to clarify the mechanism of injuries and direct clinical management [11, 12]. However, we found that the original Palmer classification system did not cover all the TFCC injuries, in line with several reports by other authors [13–17]. According to our current and previous study, we have found several traumatic injury patterns that were not included in the original Palmer classification system including capsular injuries, the horizontal tear of the articular disk, and the bucket-handle tear. As the complex anatomy and biomechanics of the DRUJ have been gradually understood, the importance of preserving a well-functioning TFCC has been learned by clinicians [18–20]. One of the crucial importance in evaluating a patient with acute TFCC injury is the presence or absence of

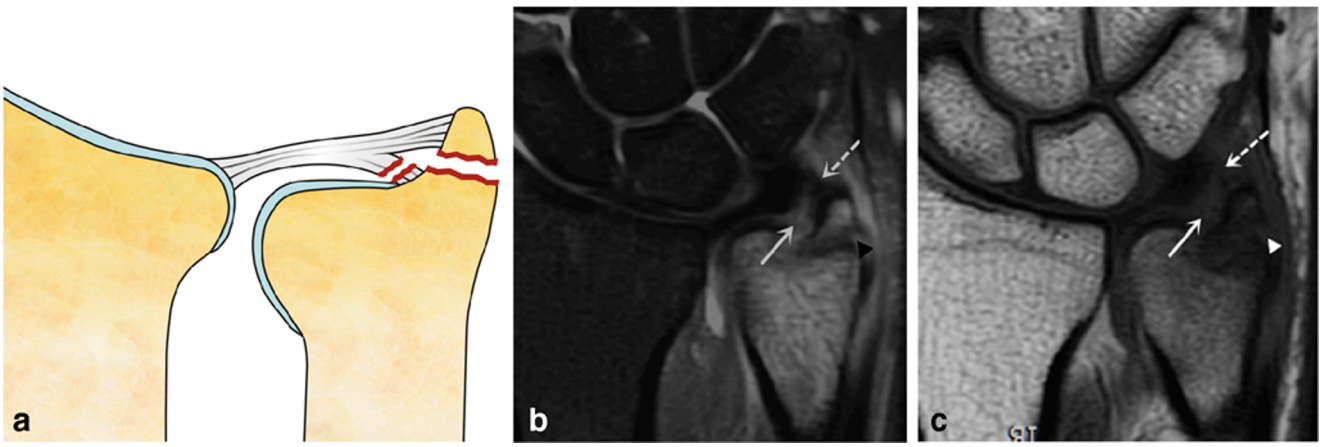

Fig. 6 IB5. Unstable pseudoarthrosis. **a** Illustration of IB unstable pseudoarthrosis showed the fracture of the ulnar styloid coupled with the foveal insertion tear. A 27-year-old female with wrist injury. **b** Coronal FS PD-weighted image and **c** T1-weighted image showed the acute fracture at the base of the ulnar styloid process (arrowhead) coupled with the proximal lamina torn (arrow) and the distal lamina was intact (dashed arrow). In addition, bone marrow edema in the ulnar styloid process, fovea and fascial edema, and fluid accumulation could also be observed. FS, fat suppression

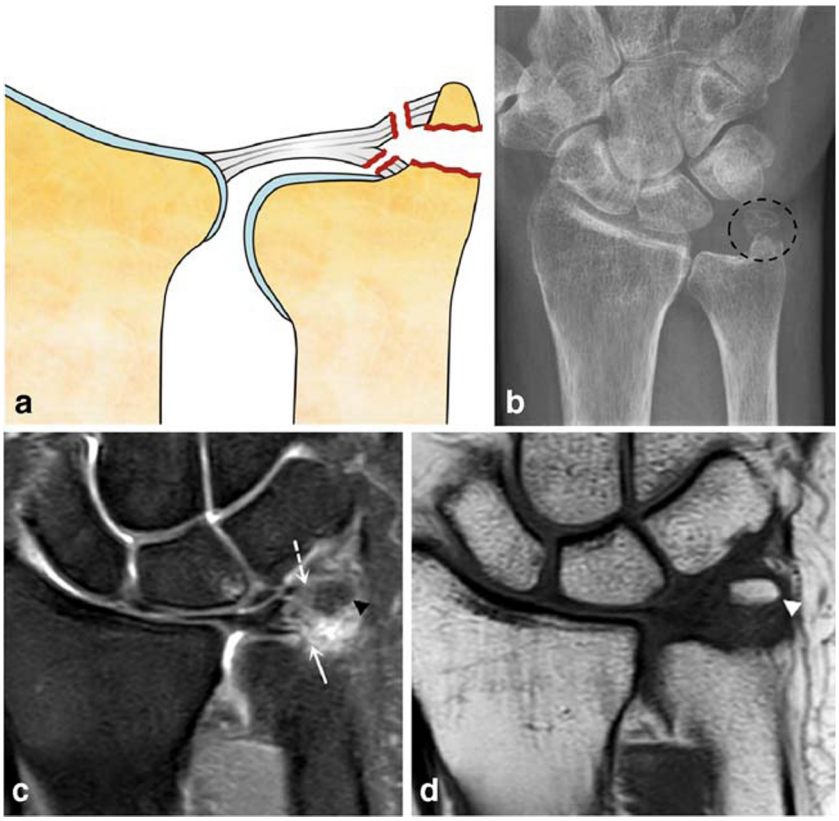

Fig. 7 IB6. Unstable pseudoarthrosis—"floating styloid". **a** Illustration of IB unstable pseudoarthrosis showed the displacement of the non-union of ulnar styloid with tear of both the foveal and styloid insertions. A 57-year-old female with wrist injury. **b** Frontal radiograph showed fracture of ulnar styloid process (dashed circle). **c** Coronal FS PD-weighted image and **d** T1-weighed image showed the moderately displaced fracture of ulnar styloid process (arrowhead). Both the proximal lamina (arrow in **c**) and distal lamina (dashed arrow in **c**) were partially torn and demonstrated as discontinuity and increased signal intensity. The slight marrow edema of the adjacent lunate could also be observed. FS, fat suppression

DRUJ instability. Biomechanical studies have suggested that the foveal insertion of the triangular ligaments plays the most important role in the stability of the DRUJ, compared with the styloid insertion [18, 21]. This understanding has helped the clinicians to realize the importance of repairing the foveal attachment. If there is DRUJ instability, then surgical treatment is required. Because the dorsal or volar rim tear of TFC is related to the DRUJ instability [3] in patient with radial tear of the TFCC associated with severe instability of DRUJ, the rim area should be repaired. When the tear is confined within the fibrocartilage area, it just needs to be partially resected arthroscopically.

Although arthroscopy has been regarded as the gold standard by some, the method is invasive. Some injury types such as the foveal insertion tear cannot be seen directly during standard wrist arthroscopy of the radiocarpal joint. Furthermore, several studies have stated that direct MR arthrography is more sensitive and specific in the diagnosis of TFCC injuries than conventional MRI [22–24]. However, the direct MR arthrography is invasive, and the technique is complex and time-consuming [12]. A recent study has shown that most of surgically relevant pathology will be visible on high-resolution conventional MRI [25]. An accurate MR imaging protocol is valuable to detect the location and extent of

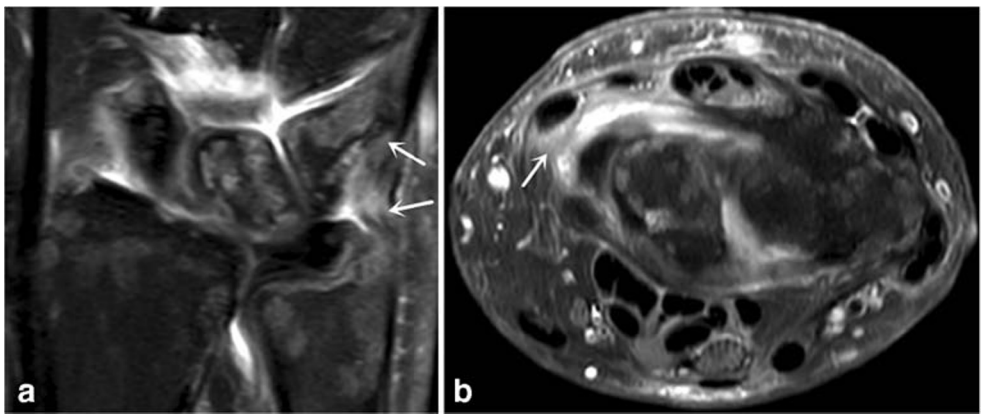

Fig. 8 Ulnomeniscal homologue tear. A 32-year-old female with wrist injury. **a**, **b** Coronal and axial FS PD-weighted images showed the meniscal homologue injury appeared as the increased signal intensity (arrow), extended from the ulnar attachment to the triquetral attachment and the extent of injury could be best appreciated on the coronal plane. FS, fat suppression

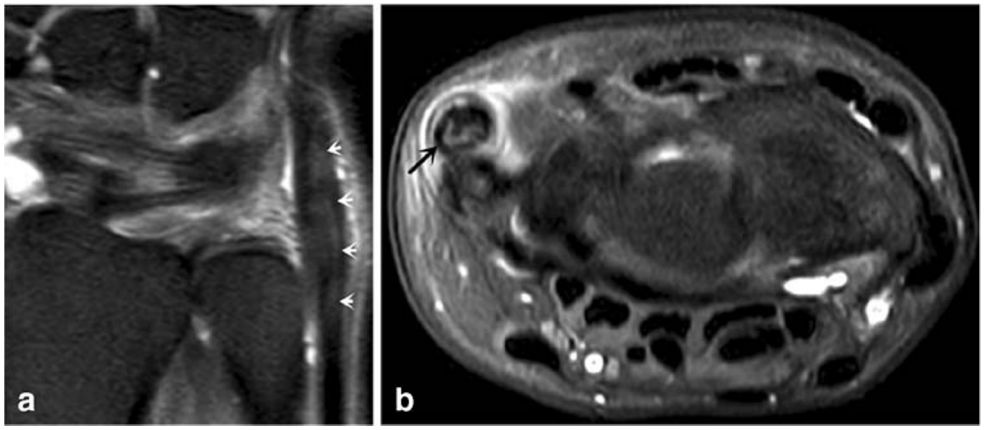

Fig. 9 Extensor carpi ulnaris (ECU) injury. A 35-year-old female with wrist injury. **a**, **b** Coronal and axial FS PD-weighted images showed intermediate signal intensity within the ECU, the enlargement of the tendon (arrowhead in **a** and arrow in **b**), tenosynovitis, and fascial edema. FS, fat suppression

injury. Currently, most surgeons often rely on MR findings and clinical data to determine whether patients should be managed conservatively or surgically. However, diagnosis for the radial side tear and the capsular detachment with lower sensitivity (67% and 20%, respectively) with different readers showed different diagnostic accuracy values for the capsular detachment (0.60 and 0.90, respectively), which may be related to the lack of knowledge of these types of injuries. Thus, it is necessary to refine and supplement the original Palmer classification system to provide a more comprehensive classification scheme and provide guidelines for clinical management.

Based on clinical, radiographic, and arthroscopic findings, Atzei described a treatment-orientated classification of TFCC peripheral tears [26–28]. However, the main focus of the paper was emphasis on the clinical management and did not display the MR features of the peripheral tears in detail. In some researches, Atzei-EWAS classification was used to categorize the peripheral tears of TFCC [29, 30]. Thus, a clinically relevant and detailed classification of TFCC injury can not only improve the communication between clinicians and radiologists but also provide reference for the preoperative planning. On the basis of Atzei's classification system, we recommended subdividing Palmer IB injuries as ulnar attachment injuries and miscellany (Table 1). We believe that this subdivision of type IB injuries could provide more insights into the treatment strategies. For example, non-surgical treatment is sufficient for patients with TFCC tears without DRUJ instability. In our study, the foveal insertion tear was relatively more

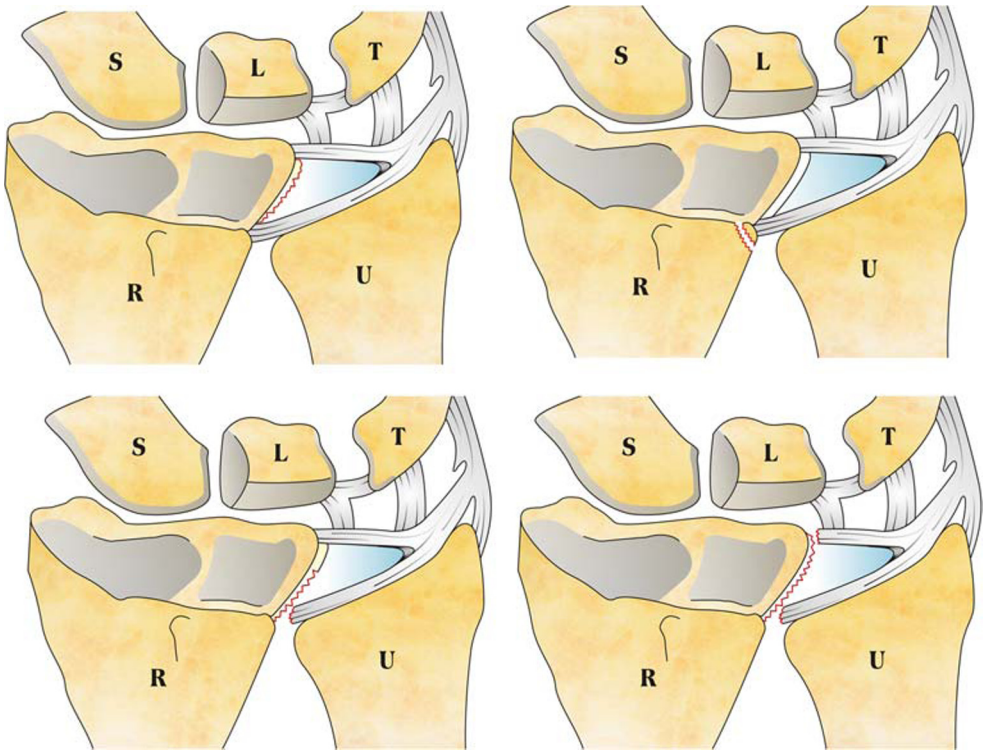

Fig. 10 ID. Refined classification of radial avulsion of TFCC. Schematic drawings, displaying from the dorsal view and looked down, showed the radial avulsion could be subdivided as follows: fibrocartilage tear between the hyaline cartilage of the sigmoid notch of the radius and TFC; dorsal/volar rim tear between the dorsal/volar edge of the radial sigmoid notch and the dorsal/volar distal radioulnar ligament with/without avulsion fracture of the dorsal/volar margin of the radial sigmoid notch; fibrocartilage-radius interface tear coupled with rim tear; and the total avulsion of the TFCC from the radius. S, scaphoid; L, lunate; T, triquetrum; R, radius; U, ulna

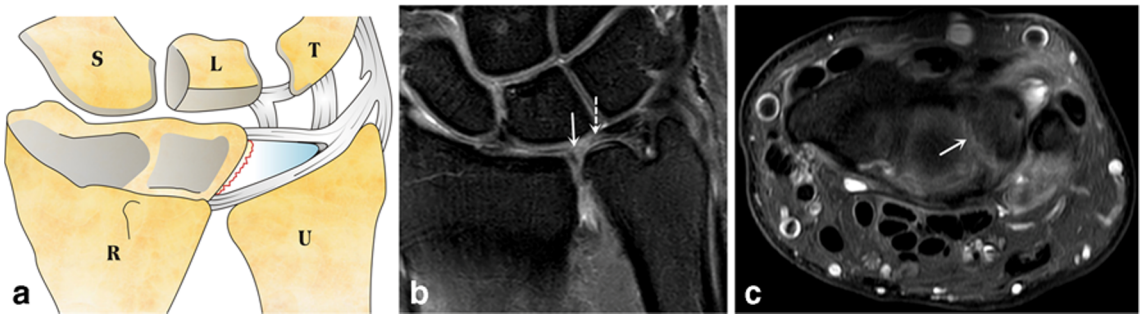

Fig. 11 ID1. Fibrocartilage-radius interface tear. **a** Illustration of the fibrocartilage-radius interface tear. S, scaphoid; L, lunate; T, triquetrum; R radius; U, ulna. A 65-year-old male with wrist injury. **b**, **c** Coronal and axial FS PD-weighted images illustrated the avulsion of the TFC radial attachment (arrow) between the hyaline of the radial sigmoid notch and TFC with peripheral retraction of the TFC (dashed arrow) leaving a gap. FS, fat suppression

common than other types, which is not in accordance with the literature [28]. The literature said the complete tear is the commonest symptomatic peripheral TFCC tear, and we think the discrepancy may be due to the small sample size in our study.

The radial tears of the TFCC include fibrocartilage-radius interface tear, dorsal/volar rim tear with/without avulsion fracture of the sigmoid notch of the radius, compound injury of fibrocartilage tear, and rim avulsion and total avulsion. Axial images are useful and the consecutive coronal images could also be helpful to detect this type of injury. Because this type of tear with dorsal or volar rim involvement is associated with DRUJ instability, it is of importance to differentiate the location and extent of this type of injury. It is necessary to repair the rim area for the radial tear of the TFCC with DRUJ instability. On the other hand, the tear confined within the fibrocartilage just needs arthroscopic partial resection. There were only 3 cases of radial attachment injuries proven by arthroscopy or surgery; no dorsal avulsion of the sigmoid notch of the radius and total avulsion is found in our study. We think there are reasons that can account for it. First of all, these subtype injuries of radial attachment are uncommon; especially the surgeons may miss the small slit on the radiocarpal arthroscopy or at times the rim tear is difficult to assess from the arthroscopic exploration. On the other hand, if there are no signs of DRUJ instability, no arthroscopic exploration or surgery is necessary.

There are 4 bucket-handle tears of the TFCC confirmed by arthroscopy or surgery in our study. This type of injury was only seen in two case reports in the literature [31, 32]. In our study, there were two radial tears with partial avulsion of the distal radioulnar ligaments from the articular disk. This was

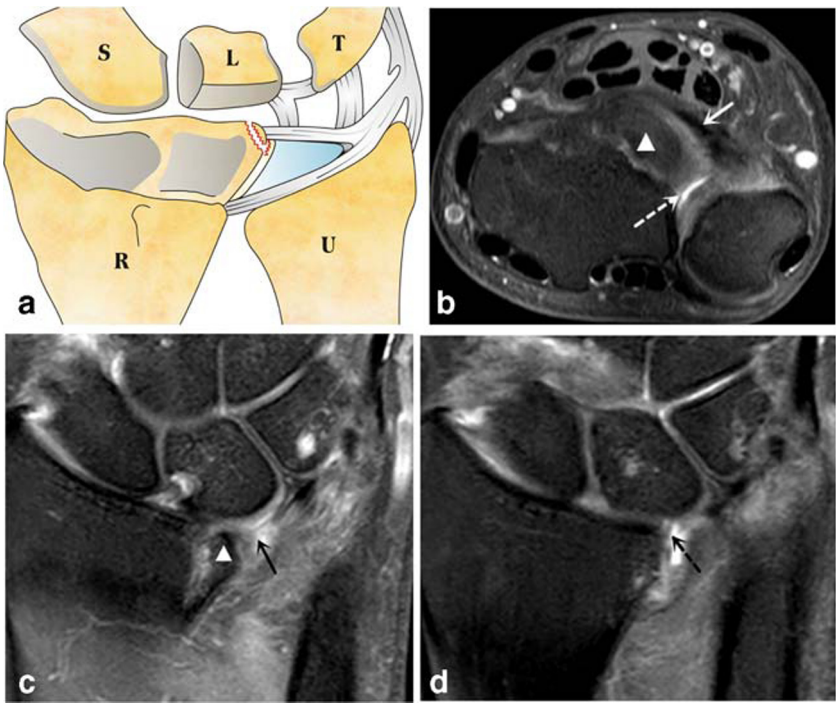

Fig. 12 ID3. Fibrocartilage tear + volar rim tear with avulsion fracture of the radial sigmoid notch. **a** Illustration of the combined injury showed the radial TFC tear and volar distal radioulnar ligament avulsion of the TFCC from the sigmoid notch of the radius coupled with the avulsion fracture. S, scaphoid; L, lunate; T, triquetrum; R, radius; U, ulna. A 49-year-old female with wrist injury. **b**–**d** Axial and coronal FS PD-weighted images showed the avulsion of the fibrocartilage-radius interface (dashed arrow) and the volar distal radioulnar ligament (arrow) presented as discontinuity and high signal intensity. Note also an avulsion fracture of the radial sigmoid notch (triangular)

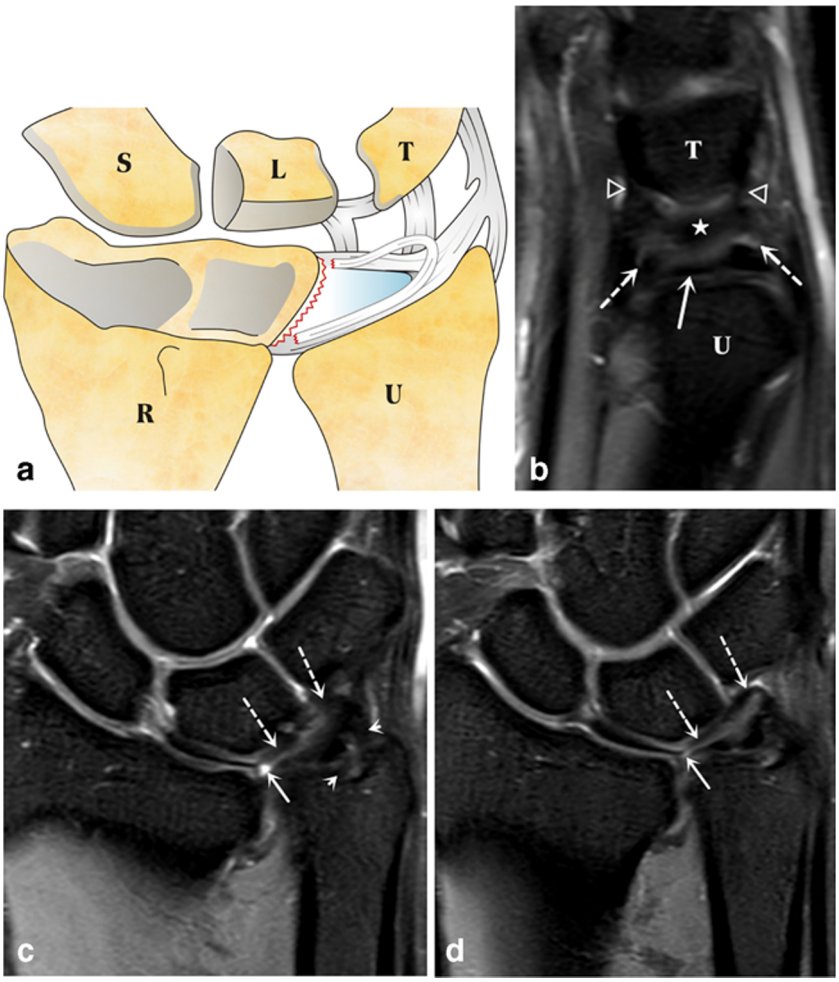

Fig. 13 Bucket-handle tear. **a** Schematic drawing of bucket-handle tear. S, scaphoid; L, lunate; T, triquetrum; R, radius; U, ulna. A 29-year-old male with wrist injury. **b** Sagittal FS PD-weighted image illustrated partial separation of the volar and dorsal distal radioulnar ligaments (dashed arrow) from the articular disk (arrow). The volar and dorsal ulnotriquetral ligaments were intact (arrowhead), and the fragment (asterisk) located between the preserved articular disk (arrow) and the triquetrum (T). **c**, **d** Coronal FS PD-weighted images showed the radial avulsion (arrow) from the hyaline cartilage of the radial sigmoid notch and the fragment (dashed arrow) located between the preserved articular disk and the proximal lunate and triquetrum. Note both the proximal lamina and distal lamina were intact (arrowhead). FS, fat suppression

different from the previous reports. We found the bucket-handle tear could be best appreciated on the coronal and sagittal planes with the sagittal images that were able to show additional injuries. This is consistent with a prior report in the literatures [32].

Although direct MR arthrography is reported as the most sensitive and specific imaging modality for the diagnosis of wrist ligament tears [33], a clear advantage of direct MR arthrography over the indirect MR arthrography has not been presented [34]. The direct MR arthrography is an invasive procedure. Thomsen et al. [34] have found that indirect MR arthrography was better than MRI in the diagnosis of Palmer IB tears. Therefore, all patients with clinically suspected ulnar-sided TFCC tear would undergo indirect MR arthrography. It was proven to be valuable to detect the ulnar detachment with the contrast diffused from synovia into the joint space where it created the direct arthrographic effect with contrast media in the joint space. However, further study is necessary about the diagnostic performance of indirect MR arthrography in the diagnosis of TFCC injuries because of the small sample of arthrography in our study.

There are limitations in our study. Because the purpose of our study was to list a TFCC injury classification as comprehensively as possible, including those not requiring surgery, we enrolled patients who had follow-up data instead of surgery. And some patients with traumatic TFCC injuries may not need the arthroscopic exploration if they do not have severe DRUJ instability. This type of injury just needs to be immobilized in a cast for at least 6 weeks. Therefore, the sample size with arthroscopic verification is small. The small sample size may be part of the reasons for the lower sensitivity and accuracy in the diagnosis of capsular detachment (P value > 0.05). In addition, for patients with conservative treatment, we can only confirm our diagnosis according to the signal changes or the relief of symptoms.

Conclusions

In conclusion, high-resolution 3-T MRI with/without arthrography is the most valuable for preoperative diagnosis of TFCC injuries. Although the original Palmer classification has been proven to be useful in the diagnosis and treatment of

TFCC injuries, with high-resolution 3-T MRI, we have found more subtype injuries and we feel it is necessary to refine the original Palmer classification to provide comprehensive guidelines for clinical management and preoperative planning.

Funding information This study was funded by the National Natural Science Foundation of China (grant number 81771809, 81371515), the Beijing Natural Science Foundation of China (grant number 7202063, 7142075), the Capital Medical Development and Scientific Research Fund of China (grant number 2016-2-1122).

Compliance with ethical standards

Conflict of interest The authors declare that they have no conflict of interest.

Ethical approval All procedures performed in studies involving human participants were in accordance with the ethical standards of the institutional and/or national research committee and with the 1964 Helsinki declaration and its later amendments or comparable ethical standards.

Informed consent Informed consent was obtained from all individual participants included in the study.

References

1. Nakamura T, Yabe Y, Horiuchi Y. Functional anatomy of the triangular fibrocartilage complex. J Hand Surg (Br). 1996;21(5):581–6.
2. Nakamura T, Yabe Y. Histological anatomy of the triangular fibrocartilage complex of the human wrist. J Ann Anat. 2000;182(6):567–72. https://doi.org/10.1016/S0940-9602(00)80106-5.
3. Cerezal L, de Dios B-MJ, Canga A, et al. MR and CT arthrography of the wrist. Semin Musculoskelet Radiol. 2012;16(1):27–41. https://doi.org/10.1055/s-0032-1304299.
4. Cerezal L, Abascal F, García-Valtuille R, Del Piñal F. Wrist MR arthrography: how, why, when. Radiol Clin North Am. 2005;43(4):709–31. https://doi.org/10.1016/j.rcl.2005.02.004.
5. Ahn AK, Chang D, Plate AM. Triangular fibrocartilage complex tears: a review. Bull NYU Hosp Jt Dis. 2006;64(3–4):114–8.
6. Palmer AK, Werner FW. The triangular firocartilage complex of the wrist-anatomy and function. J Hand Surg [Am]. 1981;6(2):153–62.
7. Linscheid RL. Biomechanics of the distal radioulnar joint. Clin Orthop Relat Res. 1992;275:46–55.
8. Moser T, Dosch JC, Moussaoui A, Dietemann JL. Wrist ligament tears: evaluation of MRI and combined MDCT and MR arthrography. AJR Am J Roentgenol. 2007;188(5):1278–86. https://doi.org/10.2214/AJR.06.0288.
9. Lee RK, Ng AW, Tong CS, et al. Intrinsic ligament and triangular fibrocartilage complex tears of the wrist: comparison of MDCT arthrography, conventional 3-T MRI, and MR arthrography. Skelet Radiol. 2013;42(9):1277–85. https://doi.org/10.1007/s00256-013-1666-8.
10. Zhan H, Zhang H, Bai R, et al. High-resolution 3-T MRI of the triangular fibrocartilage complex in the wrist: injury pattern and MR features. Skelet Radiol. 2017;46(12):1695–706. https://doi.org/10.1007/s00256-017-2739-x.
11. Oneson SR, Scales LM, Timins ME, Erickson SJ, Chamoy L. MR imaging interpretation of the Palmer classification of triangular fibrocartilage complex lesions. RadioGraphic. 1996;16(1):97–106. https://doi.org/10.1148/radiographics.16.1.97.
12. Cody ME, Nakamura DT, Small KM, Yoshioka H. MR imaging of the triangular fibrocartilage complex. Magn Reson Imaging Clin N Am. 2015;23(3):393–403. https://doi.org/10.1016/j.mric.2015.04.001.
13. Skalski MR, White EA, Patel DB, Schein AJ, RiveraMelo H, Matcuk GR Jr. The traumatized TFCC: an illustrated review of the anatomy and injury patterns of the triangular fibrocartilage complex. Curr Probl Diagn Radiol. 2016;45(1):39–50. https://doi.org/10.1067/j.cpradiol.2015.05.004.
14. Daunt N. Magnetic resonance imaging of the wrist: anatomy and pathology of interosseous ligaments and the triangular fibrocartilage complex. Curr Probl Diagn Radiol. 2002;31(4):158–76.
15. Morisawa Y, Nakamura T, Tazaki K. Dorsoradial avulsion of the triangular fibrocartilage complex with an avulsion fracture of the sigmoid notch of the radius. J Hand Surg Eur Vol. 2007;32(6):705–8. https://doi.org/10.1016/J.JHSE.2007.06.008.
16. Estrella EP, Hung LK, Ho PC, Tse WL. Arthroscopic repair of triangular fibrocartilage complex tears. J Arthrosc. 2007;23(7):729–737.e1. https://doi.org/10.1016/j.arthro.2007.01.026.
17. Abe Y, Moriya A, Tominaga Y, Yoshida K. Dorsal tear of triangular fibrocartilage complex: clinical features and treatment. J Wrist Surg. 2016;5(1):42–6. https://doi.org/10.1055/S-0035-1570037.
18. Haugstvedt JR, Berger RA, Nakamura T, Neale P, Berglund L, An KN. Relative contributions of the ulnar attachments of the triangular fibrocartilage complex to the dynamic stability of the distal radioulnar joint. J Hand Surg [Am]. 2006;31(3):445–51. https://doi.org/10.1016/j.jhsa.2005.11.008.
19. Haugstvedt JR, Soreide E. Arthroscopic management of triangular fibrocartilage complex peripheral injury. Hand Clin. 2017;33(4):607–18. https://doi.org/10.1016/j.hcl.2017.06.005.
20. Nakamura T, Sato K, Okazaki M, Toyama Y, Ikegami H. Repair of foveal detachment of the triangular fibrocartilage complex: open and arthroscopic transosseous techniques. Hand Clin. 2011;27(3):281–90. https://doi.org/10.1016/j.hcl.2011.05.002.
21. Dy CJ, Ouellette EA, Makowski ALH, Milne E, Latta LL. Peripheral triangular fibrocartilage complex tears cause ulnocarpal instability: a biomechanical pilot study. Clin Orthop Relat Res. 2012;470(10):2771–5. https://doi.org/10.1007/S11999-012-2399-z.
22. Petsatodis E, Pilavaki M, Kalogera A, Drevelegas A, Agathangelidis F, Ditsios K. Comparison between conventional MRI and MR arthrography in the diagnosis of triangular fibrocartilage tears and correlation with arthroscopic findings. Injury. 2019;50(8):1464–9. https://doi.org/10.1016/j.injury.2019.07.032.
23. Omar NN, Mahmoud MK, Saleh WR, et al. MR arthrography versus conventional MRI and diagnostic arthroscope in patients with chronic wrist pain. Eur J Radiol Open. 2019;6:265–74. https://doi.org/10.1016/j.ejro.2019.06.003.
24. Magee T. Comparison of 3-T MRI and arthroscopy of intrinsic wrist ligament and TFCC tears. AJR Am J Roentgenol. 2009;192(1):80–5. https://doi.org/10.2214/AJR.08.1089.
25. Ng AWH, Griffith JF, Fung CSY, et al. MR imaging of the traumatic triangular fibrocartilaginous complex tear. Quant Imaging Med Surg. 2017;7(4):443–60. https://doi.org/10.21037/qims.2017.07.01.
26. Atzei A. New trends in arthroscopic management of type 1-B TFCC injuries with DRUJ instability. J Hand Surg Eur Vol. 2009;34(5):582–91. https://doi.org/10.1177/1753193409100120.
27. Atzei A, Luchetti R. Foveal TFCC tear classification and treatment. Hand Clin. 2011;27(3):263–72. https://doi.org/10.1016/j.hcl.2011.05.014.

28. Atzei A, Luchetti R, Garagnani L. Classification of ulnar triangular fibrocartilage complex tears. A treatment algorithm for Palmer type IB tears. J Hand Surg Eur Vol. 2017;42(4):405–14. https://doi.org/10.1177/1753193416687479.
29. Park JH, Kim D, Park JW. Arthroscopic one-tunnel transosseous foveal repair for triangular fibrocartilage complex (TFCC) peripheral tear. Arch Orthop Trauma Surg. 2018;138(1):131–8. https://doi.org/10.1007/s00402-017-2835-3.
30. Park JH, Ahn KS, Chang A, Kwon YW, Choi IC, Park JW. Changes in the morphology of the triangular fibrocartilage complex (TFCC) on magnetic resonance arthrography related to disruption of ulnar foveal attachment. Skelet Radiol. 2019;49(2):249–56. https://doi.org/10.1007/s00256-019-03278-x.
31. Theumann N, Kamel EM, Bollmann C, Sturzenegger M, Becce F. Bucket-handle tear of the triangular fibrocartilage complex: case report of a complex peripheral injury with separation of the distal radioulnar ligaments from the articular disc. Skelet Radiol. 2011;40(12):1617–21. https://doi.org/10.1007/s00256-011-1269-1.
32. Jean J, Azael A, Barrera CM, Ezuddin NS, Chen D. MRI findings in bucket-handle tears of the triangular fibrocartilage complex. Skelet Radiol. 2018;47(3):419–24. https://doi.org/10.1007/s00256-017-2796-1.
33. Pahwa S, Srivastava DN, Sharma R, Gamanagatti S, Kotwal PP, Sharma V. Comparison of conventional MR and MR arthrography in the evaluation wrist ligament tears: a preliminary study. Indian J Radiol Imaging. 2014;24(3):259–67. https://doi.org/10.4103/0971-3026.137038.
34. Thomsen NOB, Besjakov J, Björkman A. Accuracy of pre- and postcontrast, 3T indirect MR arthrography compared with wrist arthroscopy in the diagnosis of wrist ligament injuries. J Wrist Surg. 2018;7(5):382–8. https://doi.org/10.1055/s-0038-1661419.